molecular pharmaceutics

Article

pubs.acs.org/molecularpharmaceutics

Effects of the Microparticle Shape on Cellular Uptake

Yuanzu He and Kinam Park*

Departments of Biomedical Engineering and Pharmaceutics, Purdue University, West Lafayette, Indiana 47907, United States

ABSTRACT: Physical forms of microparticles and nanoparticles, such as the size, charge, and shape, are known to affect endocytosis. Improving the physical designs of the drug carriers can increase the drug uptake efficiency and the subsequent drug efficacy. Simple shapes, such as sphere and cylinder, have been studied for their ability for endocytosis. To have a better understanding of the shape effect on cellular uptake, different particle shapes were prepared, using the keyboard character shapes, and their impacts on cellular uptake were examined. The results showed that shapes with higher aspect ratios and sharper angular features have a higher chance of adhering to the cells and become internalized by the cancer cells. The local interaction between the cell membrane and the part of the microparticle in contact with the cell membrane also plays a crucial role in determining the outcome.

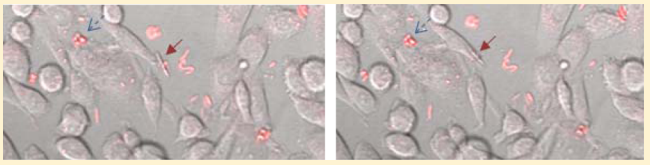

KEYWORDS: *microparticle shape, size, aspect ratio, endocytosis, cellular uptake*

1. INTRODUCTION

The physicochemical properties of drug molecules, such as size, shape, and charge, have been shown to influence the rate of diffusion through cells.[1] The properties of nano/microparticles also play an important role in cell adhesion, which is the first step to endocytosis of particles.[2,3] The physical properties (size and shape), surface properties (charge and hydrophilicity), and mechanical properties (stiffness) of particles are all known to affect endocytosis.[4−7] Exploring and understanding the relationships between particle properties and endocytosis can increase the efficiency of drugs entering cancer cells by improving the particle design. An improved drug influx into the cancer cells can increase the concentration of drug buildup inside the cells, making chemotherapy more effective. Improved delivery efficiency can also reduce the amount of cytotoxic drug needed to be administered to the patient, making chemotherapy less harmful.

Studies have suggested that a smaller diameter allows the microsphere to adhere to cells faster and more strongly.[8,9] Since strong adhesion between the nanoparticles and the cells is required for cells to internalize the nanoparticles, a smaller particle size would also imply that there is a higher chance that the nanoparticles can be internalized by cells.[10] Other studies have suggested that smaller size particles directly contribute to faster internalization by cells.[11,12] Microrod particles were more effective in triggering nonspecific cellular uptake with increased apoptotic signal and proliferation inhibition, as compared with spherical particles.[13] After endocytosis, different particles are known to spatially segregate in the cytoplasm based on their size and shape.[14,15] A study with various sizes (0.1−10 μm) and shapes (spheres vs elliptical disks) indicates that spheres were endocytosed more rapidly, while disks circulated in the blood longer with higher targeting specificity in mice.[16] Anisotropic polymeric particles, produced by the thin film stretching procedure, showed their ability to evade nonspecific cellular uptake with subsequent enhanced targeted cellular uptake and interaction.[17]

The aspect ratio of the particles is known to be important in cellular uptake. Cylindrical or rod particles in micrometer sizes were internalized better than the cubical or spherical particles of similar volume.[18,19] Among the cylindrical shaped microparticles, the high aspect ratio cylindrical microparticles had up to 4 times faster internalization rate than the low aspect ratio cylindrical microparticles.[18] Another study, however, found that lower aspect ratio nano/microparticles had better uptake.[20,21] The different results may be due to the fact that those studies used different materials and surface properties, confounding effects in the cellular response. The local shape where the particle comes in contact with the cell and the angle of the local shape play an important role in whether the particles can be internalized. It has been shown that high curvature regions contribute to particle phagocytosis.[22] Previous findings also suggest that the angle of the nanoparticle tangential to the cells or the orientation of the nanoparticles determines whether the phagocytosis would occur.[23] These findings suggest that not only the overall shape of the nanoparticles affects cellular uptake but also the part of the shape of nanoparticle that initially contacts the cell plays a major role in whether the nanoparticles will be internalized.

The surface properties, such as charge and hydrophilicity/hydrophobicity, of particles play a role in cellular uptake. Since the cell membrane is negatively charged, positively charged particles are expected to have a strong adhesion to the cell membrane due to electrostatic attraction, as long as the surface

Special Issue: Physics-Inspired Micro/Nanotherapeutics

Received: December 31, 2015
Revised: February 18, 2016
Accepted: February 23, 2016
Published: February 23, 2016

DOI: 10.1021/acs.molpharmaceut.5b00992
Mol. Pharmaceutics 2016, 13, 2164−2171

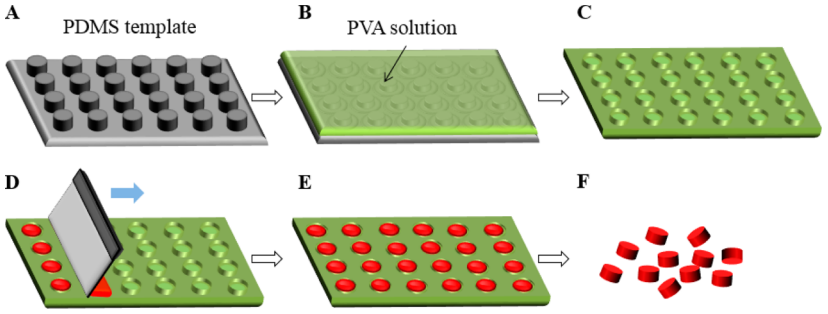

Figure 1. A schematic of polymeric microparticle fabrication process. (A) PDMS template with protrusions in the shape of keyboard characters. (B) PVA film (mold) on top of the PDMS template. (C) The dried PVA film was peeled away from the PDMS template and placed on a flat surface to expose empty microcavities. (D) Filling the wells in the mold with PLGA/Nile red solution. (E) Drying the microparticles. (F) Collecting microparticles by dissolving the PVA mold in water.

is not covered by blood proteins. Cationic particles such as poly-L-lysine, polyethylenimine, transferrin, and chitosan have been used to coat the surface of the nanoparticles to increase adhesion to cells in in vitro cell culture studies. Cellular uptake of microparticles by neuron-like PC-12 cells was studied to examine the effect of hydrophilic (Tween 80 and Triton X100) and hydrophobic (Span 80) surfactants. The in vitro study showed that more hydrophilic particles showed higher cellular uptake efficiency.[24] The mechanical properties are also known to affect cellular uptake. Soft particles with low stiffness were shown to be transported faster to lysosomes than stiffer ones.[25]

The goal of this study was to examine the effect of different shapes of microparticles on cellular uptake in a qualitative manner using shapes that were not tested before. Microparticles of different shapes and sizes were prepared using micro-fabricated keyboard characters.[26] Keyboard characters were chosen because there are various shapes and sizes that can be tested for cellular uptake without any further manipulation of the shapes.

2. MATERIALS AND METHODS

2.1. Preparation of Microparticles of Keyboard Characters. Microparticles were fabricated based on the water-soluble polymer film, also known as the hydrogel template, method developed in our laboratory.[26−28] Figure 1 shows an overall process. Keyboard characters were patterned on a silicon wafer.[26] Then, an intermediate template of poly(dimethylsiloxane) (PDMS) with the protruded characters was made from the silicon wafer master template (Figure 1A). A clear poly(vinyl alcohol) (PVA) solution was then poured on top of the PDMS template and dried to form a film with wells in the shapes patterned on the PDMS template (Figure 1B). The PVA film was peeled away from the PDMS template and placed on a flat surface to expose microcavited wells (Figure 1C). Poly(lactic-*co*-glycolic acid) (PLGA) polymer was dissolved in solvent along with Nile red dye (Sigma-Aldrich, St. Louis, MO). The mixture was then pipetted onto the PVA film surface and spread into the wells using a thin razor (Figure 1D). After drying at room temperature or in an oven (Figure 1E), the microparticles were freed by dissolving the PVA mold in Nanopure water with gentle shaking of the mixture. The free microparticles were collected by centrifugation (Figure 1F).

2.2. Fabrication of Silicon Wafer Master Template. To make a silicon wafer master template, a blank silicon wafer disk was spin coated with photoresist (MicroChem, Westborough, MA) at a set rpm for 30 s followed by baking at 95 °C for 3 min. The baked silicon wafer was exposed to UV radiation through a chromium mask containing the micrometer size keyboard patterns for a period of time using Karl Suss Mask Aligner (SUSS MicroTec AG, Germany). After UV radiation, the photomask was postbaked at 95 °C for 3 min. The silicon wafer was then soaked in a developer solution (MicroChem) and sonicated in a Branson 5200 Ultrasonic Cleaner (Branson, Danbury, CT) to dissolve away the un-cross-linked photoresist regions blocked by the chromium mask patterns during UV radiation. The cross-linked region, which was not covered by the patterns, was not dissolved by the developer solution. Dissolving of the un-cross-linked photoresist leaves wells in the shapes of the mask patterns. For the final step, the silicon wafer was rinsed with isopropanol and dried with nitrogen gas. The depth of the photoresist was controlled by the rotation speed of the spin coater, UV exposure time, and time in the developer solution. The manufactured silicon wafer master template could be used repeatedly for producing intermediate PDMS templates.

2.3. PDMS Template Fabrication. Once the silicon wafer master template was made, it was secured onto a flat glass plate by glue. The glass was then placed inside a pan for filling the PDMS gels. To make one PDMS template, 60 mL of Sylgard 184 silicone elastomer base (Ellsworth Adhesives, Germantown, WI) was mixed with 6 mL of Sylgard 184 silicone elastomer initiator (Ellsworth Adhesives). After stirring the mixture for 1 min, PDMS was poured into the pan to allow the mixture to cover the entire pan including the silicon wafer surface. The PDMS loaded pan was then placed inside a Laboport vacuum pump (KNF, Trenton, NJ) to aspirate bubbles trapped inside the PDMS. After all the bubbles were removed, the PDMS loaded pan was placed inside an oven at 60 °C for 2 h to solidify the PDMS gel. The finished PDMS was peeled and cut out of the pan and placed on a flat surface (Figure 1A).

2.4. Poly(vinyl alcohol) (PVA) Film (Mold) Fabrication. PVA with molecular weight of 146,000−186,000 Da, 99+% hydrolyzed (PVA, Sigma-Aldrich) was dissolved in a combination of deionized water and ethanol. Different concentrations of PVA and different water to ethanol ratios were tested to determine the best quality of film for polymer filling with fast solvent evaporation time. The PVA solution was placed inside an oven at 60 °C overnight and stirred with heat on a stirring plate the next day to completely dissolve the PVA.

The PVA solution was then pipetted onto the PDMS template (Akina, Inc., West Lafayette, IN) with desired protruding patterns on the surface. The PVA solution was spread onto the PDMS template surface by gently rocking the

DOI: 10.1021/acs.molpharmaceut.5b00992
Mol. Pharmaceutics 2016, 13, 2164−2171

glass slide holding the wafer (Figure 1B). Once the PVA solution was spread evenly on the template, the template was then transferred to an oven and heated at 60 °C. The PVA solution on the PDMS template was checked every 5−10 min for at least the first hour to make sure the PVA solution did not aggregate in small islands or form bubbles. A pipet tip or a thin razor can be applied to spread the film and to eliminate the bubbles. Solvent was evaporated under elevated temperature leaving only the dry PVA film. Upon drying, the PVA film could be peeled off from the PDMS template surface and placed on a flat surface to expose keyboard characters (Figure 1C). The patterns would be imprinted as wells on the film surface with the desired shapes ready for filling.

2.5. Polymer Filling and Collection. Three types of polymers have been used for filling the PVA film: PLGA (L:G = 50:50, inherent viscosity of 0.55−0.75 dL/g, Durect, Cupertino, CA), polycaprolactone (PCL, M_n = 10,000−15,000 Da, AP113, Akina, Inc.), and polystyrene (PS, M_w = 35,000 Da, Sigma-Aldrich). Polymers were dissolved in dichloromethane (DCM, VWR International, Radnor, PA), a mixture of ethyl acetate (VWR International) and benzyl alcohol (VWR International), or a mixture of DCM and benzyl alcohol. The solvent was mixed with the polymer and left at room temperature overnight to completely dissolve the polymers. Once the polymers were dissolved in the solvent, small quantities of Nile red solution was added to the polymer solution to fluorescently label the polymer.

The PVA film was stretched and secured onto a glass slide by tape. Polymer solution tagged with Nile red dye was pipetted onto one side of film in a line. A thin razor was applied to swipe the solution on the PVA film surface back and forth several times, allowing the polymer to fill the wells on the film (Figure 1D). The number of swipes performed depended on the evaporation rate of the polymer solvent. The entire process was repeated on the same PVA film once or twice with a new razor each time for better polymer filling efficiency.

Once the polymer solution was dried (Figure 1E), the polymer-filled portion of the PVA film was cut out and dissolved in deionized water. Deionized water dissolved the PVA film, leaving only the free polymer microparticles (Figure 1F). The polymer/deionized water mixture was then filtered through a fine molecular sieve or filter paper to obtain pure microparticles. The final collected microparticle solution was either used for experiments immediately or frozen at −80 °C and lyophilized for future use.

2.6. Microparticle Characterization. The prepared microparticles were visualized using a fluorescent microscope and a confocal microscope at an excitation wavelength of 485 nm. The microparticles were examined right after PVA filling, where the microparticles still remained in the PVA film wells, as well as after collecting free microparticles. The free microparticles were also dried and examined under a scanning electron microscope (SEM). The size and shape of the microparticles were examined.

2.7. LnCAP Cell Culture. The cell line used for the microparticle endocytosis study was LnCAP cells (ATCC, Manassas, VA), which is a prostate cancer cell line. The cells were seeded in culture flasks for growing stocks or confocal culture dishes for imaging purposes. The medium used was RPMI-1640 medium (ATCC) supplemented with 10% (v/v) fetal bovine serum (FBS, Invitrogen, Carlsbad, CA) and 1% (v/v) penicillin/streptomycin (P/S, Invitrogen). The culture flask was grown in the incubator at 37 °C with 5% CO_2.

To maintain cell viability, the medium was replaced every 2 days. When the cells reached 80% confluency, the cells were resuspended using trypsin. The suspended cells were then seeded into a new culture flask at a lower concentration or a new confocal culture dish for cellular uptake imaging. To store the LnCAP cells, suspended cells were stored in complete growth medium supplemented with 5% (v/v) dimethyl sulfoxide (DMSO, Sigma-Aldrich). The solution was stored in cryogenic vials and frozen at −80 °C in a cryochamber. For the imaging study, the cells were treated with 60 μL of 0.1 mg/mL BODIPY FL C16 dye in a confocal culture dish. The confocal culture dish was then wrapped with foil and incubated at 37 °C for 1 h to allow the dye to attach to the cell membrane.

2.8. Confocal Imaging. The confocal microscope used for the cell and microparticle imaging was an inverted LSM 710 confocal microscope (Carl Zeiss AG, Germany). The platform was equipped with an incubation chamber that allowed the cells to be imaged at a maintained 37 °C, which was an ideal temperature for living cells. The confocal culture dish was fixed inside the incubation chamber. Associated Zen Light software was used to set the parameters and to control the operations of the device.

All the necessary parameters were manipulated using the Zeiss microscope software. Multiple excitation wavelengths were set to image the cell membrane dye and the microparticle tagged dye. The membrane dye boron-dipyrromethene FL C16 (BODIPY FL C16, Invitrogen) was excited at a wavelength of 600 nm, and Nile red dye was excited at a wavelength of 485 nm. The quality of the image and the speed of image taken were set as compromised in the setting option.

Z-stack function was applied. Multiple images were taken along the *z*-direction to study the cells in depth. The in-depth imaging allowed the cells and the microparticle interactions to be visualized in 3 dimensions. This was used to figure out whether the microparticle was inside the cell or just next to the cell. Time lapse images were taken continuously at a set interval of 30 s or 1 min. The total duration of study varied from 1.5 to 4 h. The cells and microparticles could be monitored continuously. Changes in positions of the same cell and same microparticle could be tracked as time progressed. Multiple positions were taken on the confocal culture dishes simultaneously. *Z*-stack parameters were different but time lapse images were the same for different positions.

3. RESULTS AND DISCUSSION

3.1. Microparticle Fabrication. Three different types of polymers were used to make microparticles. PLGA was selected because it is the most commonly used polymer for fabricating

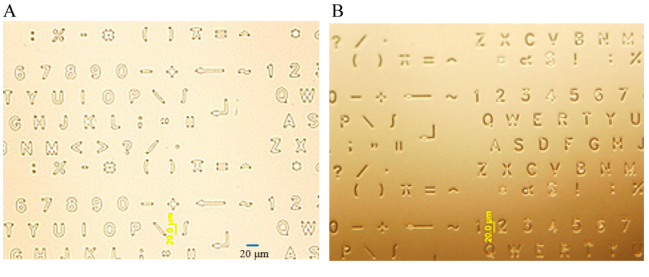

Figure 2. Bright field images of silicon wafer keyboard characters with 2 μm (A) and 10 μm (B) photoresist depth.

DOI: 10.1021/acs.molpharmaceut.5b00992
Mol. Pharmaceutics 2016, 13, 2164−2171

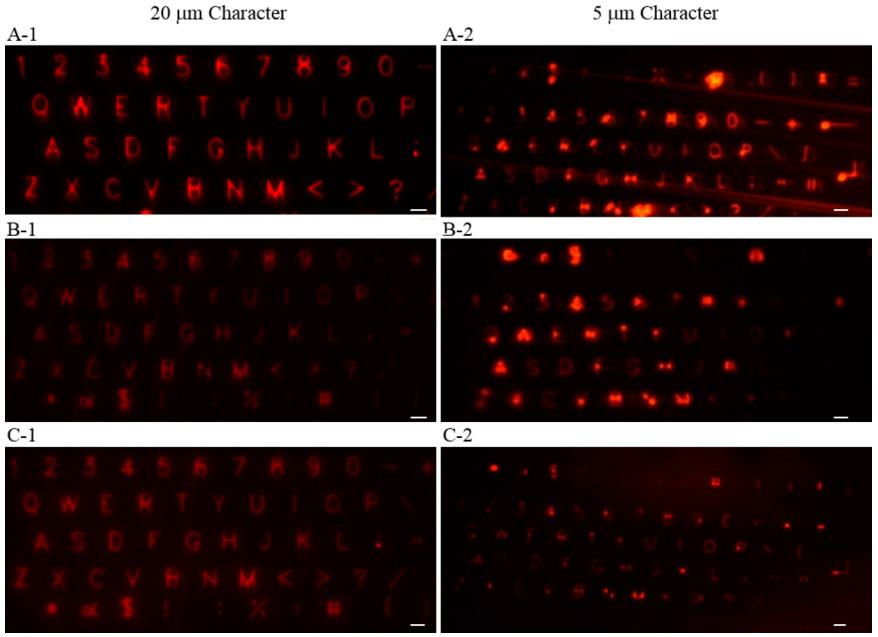

Figure 3. Fluorescent microscopic images of keyboard characters in 20 and 5 μm sizes after filling PVA molds with polymer/Nile red solution. Polymers used were 10% PLGA (A), 20% PS (B), and 50% PCL (C). Scale bar = 20 μm on the left panels and 5 μm on the right panels.

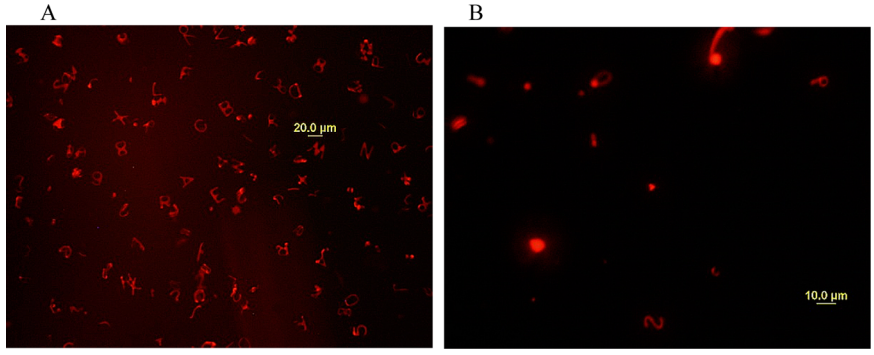

Figure 4. Fluorescent images of 20 μm (A) and 5 μm (B) PLGA microparticles.

microparticles, and it has been used in a dozen of biodegradable long-term depot formulations approved by the Food and Drug Administration (FDA). PS and PCL were used as alternative polymers.

To fabricate the silicon wafer master template with the best quality, the depth of the photoresist, the exposure time of silicon wafer to UV radiation, and the contact proximity of the chromium mask to the silicon wafer were varied to determine the optimum combinations to produce the best quality silicon wafer. Of the photoresists of different thicknesses tested (2 μm, 5 μm, and 10 μm), the 2 μm thickness showed the most clear etching pattern after UV radiation. Figure 2 shows bright field microscopic images of silicon wafer keyboard characters with 2 and 10 μm photoresist depth. There was an optimum time for UV radiation exposure at each photoresist thickness. A longer or shorter exposure time resulted in blurry patterns on the silicon wafer. This could be contributed to the under-development or overdevelopment of the photoresist. Close contact was preferred to loose contact for the space between the silicon wafer and the chromium mask. This may be due to the fact that patterns on the chromium mask could not completely prevent the photoresist underneath the patterns from exposure to the UV radiation, causing unwanted cross-linking of the photoresist underneath the patterns.

Different solvent combinations and PVA concentrations were tested to find the best quality film (or mold). Different ratios of ethanol to distilled water were tested to dissolve PVA. PVA with higher ethanol content (ethanol:water = 4:1) could evaporate and form films faster with good spreading on the PDMS template surface and fewer bubbles trapped in the film, but dissolve less PVA. The films produced tended to be blurry in some areas. The PVA with higher distilled water content (ethanol:water = 2:3) could produce better quality film but took longer to evaporate, and it was very hard to spread evenly on the PDMS template surface, leaving holes on the film. Ethanol has lower surface tension with a higher degree of wettability on the PDMS surface than distilled water. Fast evaporation of ethanol also favored escape of air bubbles from the film. The PVA film with higher ethanol content solvent tended to be blurry. This may be attributed to the fact that the PVA concentration in this type of solvent had to be low to completely dissolve all PVA, so addition of more PVA solution was required during the incubation period, causing overlapping of PVA film in some areas on the PDMS template and producing the blurry effect. A higher concentration of 4% PVA

DOI: 10.1021/acs.molpharmaceut.5b00992
Mol. Pharmaceutics 2016, 13, 2164−2171

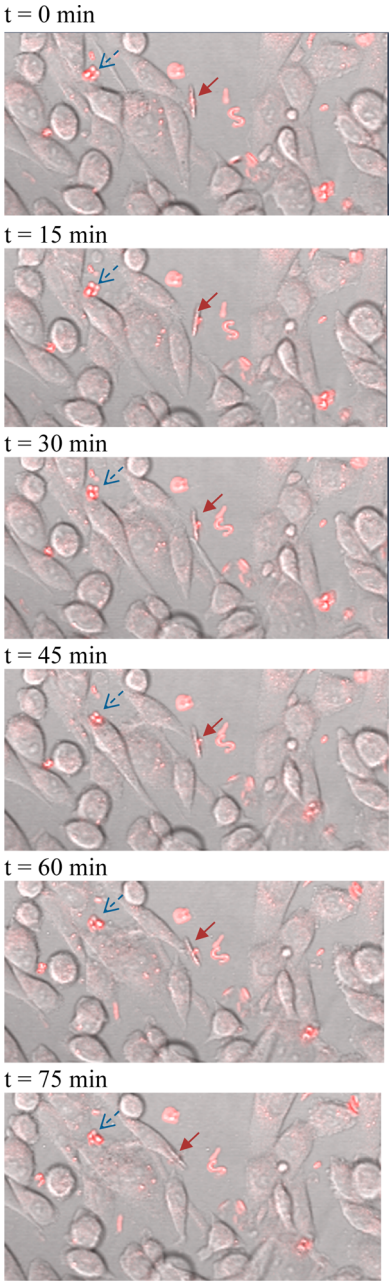

Figure 5. Uptake of 20 μm PLGA microparticles in LnCAP cells. The images were recorded on an inverted LSM 710 confocal microscope where images of the cell and microparticle interactions were recorded every minute for 1.5 h. The pound key character was not taken up by the cell after 75 min, but the backslash symbol was internalized by the cell.

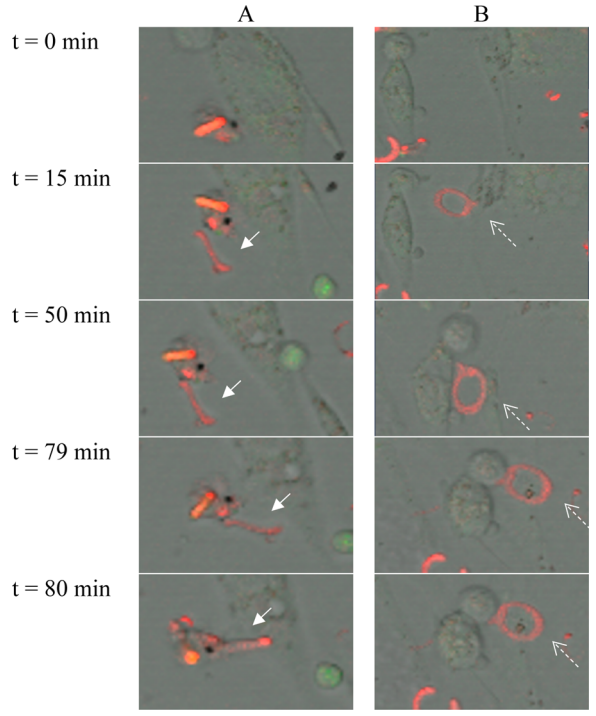

Figure 6. Internalization of PLGA keyboard microparticle in LnCAP cells. The images were recorded on an inverted LSM 710 confocal microscope where images of the cell and microparticle interactions were recorded every minute for 1.5 h. (A) One cell internalized a tilde character that was larger than the cell itself (A), while cells could not internalize letter Q (B).

solution spread more evenly on the PDMS template surface compared with lower concentration PVA solutions and also produced thicker films that were strong. However, the more concentrated PVA solution trapped more air bubbles in the film, decreasing the smoothness of the film. A lower concentration of 1% or 2% PVA solution was much harder to spread evenly on the PDMS template surface, and the films were thinner and thus were susceptible to tearing when swept, but the film had fewer bubbles, producing a smoother film. The best combination of the PVA solution was the 4% PVA initially fully dissolved in a combination of ethanol and water at the ratio of 2:3, which was then further diluted with ethanol in the ratio of 1:2. The final PVA concentration was 1.3% with a final ethanol to water ratio of 4:1. The solution spread well with minimum bubbles formed. The concentration of PVA is high enough to produce a strong PVA film that could withstand swiping.

Different solvents were used to dissolve different polymers which were used for filling the film wells. Pure DCM and a combination of ethyl acetate and benzyl alcohol or DCM and benzyl alcohol were used to dissolve the polymers. When the polymer was dissolved in a mixture of ethyl acetate and benzyl alcohol, the polymer solution could be swept on the PVA template surface over 8 times without any undesirable scum layer formation. As more DCM was added into the solvent, fewer swipes could be applied, due to the fast evaporation of DCM. All three different solvents resulted in good filling of the PVA template wells. Figure 3 shows examples of keyboard characters after filling PVA molds with different polymers. Among the three types of polymers tested, 10% PLGA had a better filling than the 20% PS and 50% PCL. Thus, subsequent studies were done using keyboard microparticles made of PLGA.

The 20 μm microparticles had a much higher yield than the 5 μm microparticles. This may be due to the fact that 5 μm microparticles had features that were submicrometer sizes, which were very fragile and susceptible to breaking under high rotation speed of the centrifugation process. Figure 4 shows 20 μm microparticles (panel A) and 5 μm microparticles (panel B). Many letters (such as B, E, H, M, O, S, T, V, X, and Y) and numbers (e.g., 5, 6, and 8) can be clearly distinguished in panel A. Letters Q and P and number 2 can be seen in panel B.

DOI: 10.1021/acs.molpharmaceut.5b00992
Mol. Pharmaceutics 2016, 13, 2164−2171

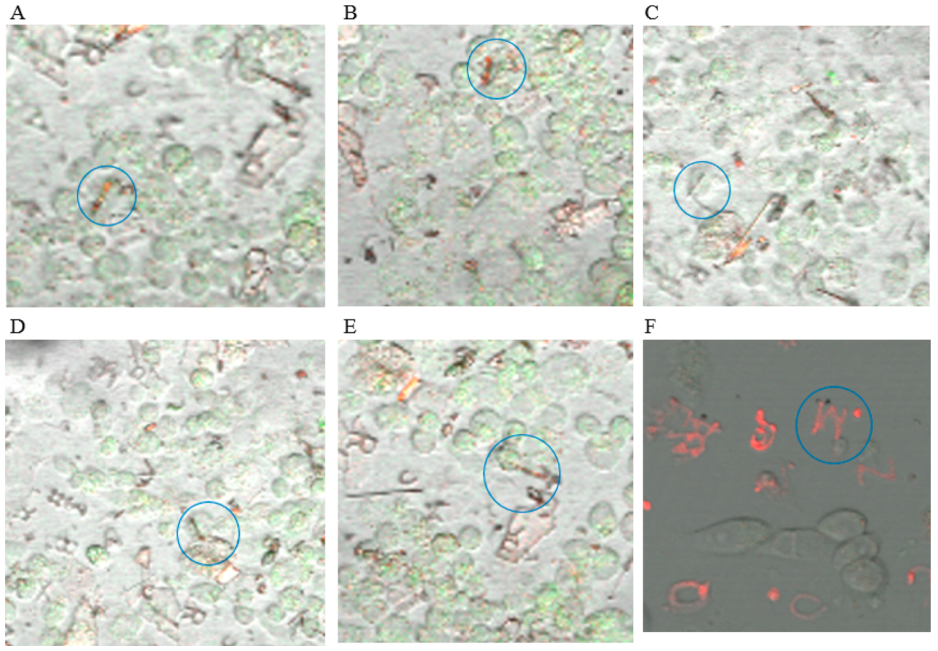

Figure 7. Interactions between cell and PLGA microparticles. Panels A to D show uptake of rodlike geometries. Panel E shows a cell trying to internalize a microparticle larger than itself. Panel F shows adhesion of the sharp end of letter M microparticle to a cell.

3.2. Cellular Uptake Study. It was difficult to make a significant amount of 5 μm microparticles, and thus, only the 20 μm microparticles were studied for the cellular uptake study. The 20 μm microparticles were introduced into a confocal dish seeded with LnCAP cells and imaged continuously for 1−3 h. As shown in Figure 5, the thinner, sharper backslash microparticle (red solid arrow) was internalized by the LnCAP cell after 75 min. On the other hand, the wider pound key character (blue dotted arrow) deformed the LnCAP membrane trying to enter the cell, but was not successful. This is similar to a previous finding that microparticle shapes with higher aspect ratios could be internalized by the cells faster.[18] There was an LnCAP cell below the backslash microparticle extending its pseudopods to try to internalize the backslash character, but it ignored the S shape microparticle that was closer in proximity from 15 to 30 min. This may be due to cells that preferred sharp edges and recruited actin filaments to wrap around the microparticles.

The results also showed that cells had the potential to internalize microparticles that were longer than the cell itself. The Figure 6A shows that the cell extended its membrane to internalize a tilde character (solid arrow) that was larger than the cell itself. One end of the tilde character was first attached to the membrane surface of the cell. The microparticle maintained the attachment for 50 min with rotation of the character from a vertical position to a more horizontal position. This could be due to the movement of either the character or the cell, or it could be due to membrane actin repositioning the direction of the tilde character for cell entry. The internalization of the microparticle happened very fast between the 80 min mark and the 81 min mark, where the cell actually became larger to internalize the microparticle. The character Q (dotted arrow in Figure 6B) had weak attachment to the cell surface as shown at 15 min with its tip end, but the entire character could not be internalized after 80 min. This may be due to the round geometry that may not be good for cell penetration as indicated by previous studies.[22]

Microparticle interactions with cells after 2 to 3 h can be divided into 3 categories: cell entry, cell surface attachment, and no entry. For the characters that had a very high aspect ratio (rodlike) shape, such as letter I, number 1, minus sign, backslash/forward slash, and tilde key, the microparticles could penetrate and enter the cancer cells completely after 2 to 3 h as shown in Figure 7 A−D. Shapes with sharp regions could attach to the surface with the sharp part of the characters. Figure 7E shows another example of a cell trying to internalize a microparticle larger than the cell itself. Figure 7F shows that even though letter M was not internalized by the cancer cell, letter M was firmly attached to the cell surface for the entire 2 h experiment. The local geometry of microparticles in contact with the cell surface was very important in determining how the cell was going to interact with the microparticles. If the flat or round part of a microparticle was in contact with the cell membrane, the particle could not attach to or penetrate the cell surface. If the sharp portion of a microparticle was in contact with the cell membrane, the particle could attach to or enter the cells. This may be due to the sharper geometries of objects making it easier for the cells to recruit actin filaments to attach and engulf the objects as opposed to the objects with a flat surface. Characters without any sharp features, such as letter D, G, O, number 0, and pound key, could not attach or penetrate the cells at all. It may be too difficult for the cells to recruit enough actin filaments and surround these characters to hold or engulf the microparticles. Overall, shapes with rodlike and sharp features seem to be more likely to adhere and become internalized by the cancer cell.

4. CONCLUSIONS AND FUTURE DIRECTIONS

There is a significant need to improve the efficiency of anticancer drug delivery into cancer cells. Physical designs of drug carriers, such as size, shape, and charge, have been examined to increase the absorption of drug carriers into cells.[29−32] Although progress has been made, studies have been limited to simple shapes. To have a better understanding of the

DOI: 10.1021/acs.molpharmaceut.5b00992
Mol. Pharmaceutics 2016, 13, 2164−2171

effect of the drug carrier shape on cellular uptake, this study examined cellular uptake of more complex shapes derived from keyboard characters. Our results indicate that rodlike characters such as letter I, number 1, and arrow key are likely to be internalized by cancer cells. Shapes with no sharp features such as letter O, number 0, and pound key could not be internalized by the cells. Cells interacted with letter Q, but were unable to internalize it probably due to the difficulty in surrounding the letter. The part of keyboard microparticles in contact with the cell membrane surface is important in determining the interactions between the microparticles and the cells. The cells have a potential to internalize microparticles that are larger than the cells themselves.

For future studies, keyboard microparticles smaller than 20 μm need to be tested. Cellular uptake studies with different sizes of keyboard microparticles will provide better understanding than the studies using simpler shapes with limited sizes. The actin filament activity in cells seems crucial for interaction and subsequent internalization of microparticles. It will be very informative to stain the actin filaments of cancer cells to track their behavior toward microparticles that come in contact with them. Shapes with sharp features seem to be able to adhere to the cancer cells better. Thus, studying shapes with a different number of sharp features, such as a triangle, hexagon, pyramid, and octahedron, could be useful for improving the shape design of a drug carrier.[33] More repetitive studies need to be performed with keyboard microparticles of different sizes and different cell types to comprehensively and accurately characterize the shape-dependent endocytosis.

The results in this research are consistent with the information in the literature, and thus, they can be used as a platform to further understand the effect of complex shape design of drug carriers on endocytosis. The information can be applied to improve the physical design of drug carriers for more efficient delivery to target cells. More efficient delivery of drugs to target cells can maximize the drug efficacy with minimal side effects.

AUTHOR INFORMATION

Corresponding Author

*Purdue University, Weldon School of Biomedical Engineering, 206 S. Martin Jischke Drive, West Lafayette, IN 47907. E-mail: kpark@purdue.edu.

Notes

The authors declare no competing financial interest.

ACKNOWLEDGMENTS

This work was supported by the National Institutes of Health through CA129287 and GM095879, and by the Showalter Research Trust Fund.

REFERENCES

(1) Minchinton, A. I.; Tannock, I. F. Drug penetration in solid tumors. *Nat. Rev. Cancer* **2006**, *6*, 583−592.
(2) Hallab, N. J.; Bundy, K. J.; O'Connor, K.; Clark, R.; Moses, R. L. Cell adhesion to biomaterials: correlations between surface charge, surface roughness, adsorbed protein and cell morphology. *J. Long-Term Eff. Med. Implants* **1995**, *53*, 209−231.
(3) Absolom, D. R.; Zingg, W.; Neumann, A. W. Protein adsorption to polymer particles: role of surface properties. *J. Biomed. Mater. Res.* **1987**, *21*, 161−171.
(4) Gupta, A. K.; Gupta, M. Cytotoxicity suppression and cellular uptake enhancement of surface modified magnetic nanoparticles. *Biomaterials* **2005**, *26* (13), 1565−1573.
(5) Mitragotri, S.; Lahann, J. Physical approaches to biomaterial design. *Nat. Mater.* **2009**, *8*, 15−23.
(6) Wang, J.; Byrne, J. D.; Napier, M. E.; DeSimone, J. M. More effective nanomedicines through particle design. *Small* **2011**, *7* (14), 1919−1931.
(7) Myerson, J. W.; Anselmo, A. C.; Liu, Y.; Mitragotri, S.; Eckmann, D. M.; Muzykantov, V. R. Non-affinity factors modulating vascular targeting of nano- and microcarriers. *Adv. Drug Delivery Rev.* **2016**, DOI: 10.1016/j.addr.2015.10.011.
(8) Patil, V. R. S.; Campbell, C. J.; Yun, Y. H.; Slack, S. M.; Goetz, D. J. Particle diameter influences adhesion under flow. *Biophys. J.* **2001**, *80* (4), 1733−1743.
(9) Lamprecht, A.; Schafer, U.; Lehr, C. M. Size-dependent bioadhesion of micro- and nanoparticulate carriers to the inflamed colonic mucosa. *Pharm. Res.* **2001**, *18* (6), 788−793.
(10) He, Q.; Zhang, Z.; Gao, Y.; Shi, J.; Li, Y. Intracellular localization and cytotoxicity of spherical mesoporous silica nano- and microparticles. *Small* **2009**, *5* (23), 2722−2729.
(11) Desai, M. P.; Labhasetwar, V.; Walter, E.; Levy, R. J.; Amidon, G. L. The mechanism of uptake of biodegradable microparticles in Caco-2 cells is size dependent. *Pharm. Res.* **1997**, *14* (11), 1568−1573.
(12) Prabha, S.; Zhou, W. Z.; Panyam, J.; Labhasetwar, V. Size-dependency of nanoparticle-mediated gene transfection: studies with fractionated nanoparticles. *Int. J. Pharm.* **2002**, *244*, 105−115.
(13) Zeng, H.; Yang, H.; Liu, X.; Shi, D.; Cao, B.; Du, C.; Ouyang, J.; Yu, L.; Wang, Y.; Liao, H. In vitro effects of differentially shaped hydroxyapatite microparticles on RAW264.7 cell responses. *RSC Adv.* **2014**, *4* (54), 28615−28622.
(14) Xu, Z. P.; Niebert, M.; Porazik, K.; Walker, T. L.; Cooper, H. M.; Middelberg, A. P. J.; Gray, P. P.; Bartlett, P. F.; Lu, G. Q. Subcellular compartment targeting of layered double hydroxide nanoparticles. *J. Controlled Release* **2008**, *130* (1), 86−94.
(15) Kolhar, P.; Mitragotri, S. Polymer microparticles exhibit size and shape dependent accumulation around the nucleus after endocytosis. *Adv. Funct. Mater.* **2012**, *22* (18), 3759−3764.
(16) Muro, S.; Garnacho, C.; Champion, J. A.; Leferovich, J.; Gajewski, C.; Schuchman, E. H.; Mitragotri, S.; Muzykantov, V. R. Control of endothelial targeting and intracellular delivery of therapeutic enzymes by modulating the size and shape of ICAM-1-targeted carriers. *Mol. Ther.* **2008**, *16* (8), 1450−1458.
(17) Meyer, R. A.; Meyer, R. S.; Green, J. J. An automated multidimensional thin film stretching device for the generation of anisotropic polymeric micro- and nanoparticles. *J. Biomed. Mater. Res., Part A* **2015**, *103* (8), 2747−2757.
(18) Gratton, S. E.; Ropp, P. A.; Pohlhaus, P. D.; Luft, J. C.; Madden, V. J.; Napier, M. E.; DeSimone, J. M. The effect of particle design on cellular internalization pathways. *Proc. Natl. Acad. Sci. U. S. A.* **2008**, *105* (33), 11613−11618.
(19) Barua, S.; Yoo, J.-W.; Kolhar, P.; Wakankar, A.; Gokarn, Y. R.; Mitragotri, S. Particle shape enhances specificity of antibody-displaying nanoparticles. *Proc. Natl. Acad. Sci. U. S. A.* **2013**, *110* (9), 3270−5.
(20) Chithrani, B. D.; Ghazani, A. A.; Chan, W. C. W. Determining the size and shape dependence of gold nanoparticle uptake into mammalian cells. *Nano Lett.* **2006**, *6* (4), 662−668.
(21) Muro, S.; Garnacho, C.; Champion, J. A.; Leferovich, J.; Gajewski, C.; Schuchman, E. H.; Mitragotri, S.; Muzykantov, V. R. Control of endothelial targeting and intracellular delivery of therapeutic enzymes by modulating the size and shape of ICAM-1-targeted carriers. *Mol. Ther.* **2008**, *16* (8), 1450−1458.
(22) Champion, J. A.; Mitragotri, S. Shape induced inhibition of phagocytosis of polymer particles. *Pharm. Res.* **2009**, *26* (1), 244−249.
(23) Champion, J. A.; Mitragotri, S. Role of target geometry in phagocytosis. *Proc. Natl. Acad. Sci. U. S. A.* **2006**, *103* (13), 4930−4934.

DOI: 10.1021/acs.molpharmaceut.5b00992
Mol. Pharmaceutics 2016, 13, 2164−2171

(24) Doolaanea, A. A.; Mansor, N. I.; Mohd Nor, N. H.; Mohamed, F. Cellular uptake of Nigella sativa oil-PLGA microparticle by PC-12 cell line. *J. Microencapsulation* **2014**, *31* (6), 600−608.
(25) Hartmann, R.; Weidenbach, M.; Neubauer, M.; Fery, A.; Parak, W. J. Stiffness-dependent in vitro uptake and lysosomal acidification of colloidal particles. *Angew. Chem., Int. Ed.* **2015**, *54* (4), 1365−1368.
(26) Acharya, G.; Shin, C. S.; McDermott, M.; Mishra, H.; Park, H.; Kwon, I. C.; Park, K. The hydrogel template method for fabrication of homogeneous nano/microparticles. *J. Controlled Release* **2010**, *141*, 314−319.
(27) Acharya, G.; McDermott, M.; Shin, S. J.; Park, H.; Park, K. Hydrogel templates for the fabrication of homogeneous polymer microparticles. *Methods Mol. Biol. (N. Y., NY, U. S.)* **2011**, *726* (Biomedical Nanotechnology), 179−185.
(28) Acharya, G.; Shin, C. S.; Vedantham, K.; McDermott, M.; Rish, T.; Hansen, K.; Fu, Y.; Park, K. A study of drug release from homogeneous PLGA microstructures. *J. Controlled Release* **2010**, *146*, 201−206.
(29) Venkataraman, S.; Hedrick, J. L.; Ong, Z. Y.; Yang, C.; Ee, P. L. R.; Hammond, P. T.; Yang, Y. Y. The effects of polymeric nanostructure shape on drug delivery. *Adv. Drug Delivery Rev.* **2011**, *63* (14−15), 1228−1246.
(30) Lin, S.-Y.; Hsu, W.-H.; Lo, J.-M.; Tsai, H.-C.; Hsiue, G.-H. Novel geometry type of nanocarriers mitigated the phagocytosis for drug delivery. *J. Controlled Release* **2011**, *154* (1), 84−92.
(31) Yameen, B.; Choi, W. I.; Vilos, C.; Swami, A.; Shi, J.; Farokhzad, O. C. Insight into nanoparticle cellular uptake and intracellular targeting. *J. Controlled Release* **2014**, *190*, 485−499.
(32) Ernsting, M. J.; Murakami, M.; Roy, A.; Li, S.-D. Factors controlling the pharmacokinetics, biodistribution and intratumoral penetration of nanoparticles. *J. Controlled Release* **2013**, *172* (3), 782−794.
(33) Jo, D. H.; Kim, J. H.; Lee, T. G.; Kim, J. H. Size, surface charge, and shape determine therapeutic effects of nanoparticles on brain and retinal diseases. *Nanomedicine* **2015**, *11* (7), 1603−1611.

DOI: 10.1021/acs.molpharmaceut.5b00992
Mol. Pharmaceutics 2016, 13, 2164−2171